BRITISH JOURNAL OF HOSPITAL MEDICINE

ARTICLE

Sensitivity of Functional Arterial Spin Labelling in Detecting Cerebral Blood Flow Changes

Qing Li[1,*], Shan Shen[2], Ming Lei[1]

[1]Department of Neurology, Wuhan Brain Hospital, General Hospital of Yangtze River Shipping, Wuhan, Hubei, China
[2]Centre for Integrative Neuroscience and Neurodynamic, University of Reading, Reading, UK
*Correspondence: icelqing@163.com (Qing Li)

Abstract

Aims/Background Arterial spin labelling (ASL) is a non-invasive magnetic resonance imaging (MRI) method. ASL techniques can quantitatively measure cerebral perfusion by fitting a kinetic model to the difference between labelled images (tag images) and ones which are acquired without labelling (control images). ASL functional MRI (fMRI) provides quantitative perfusion maps by using arterial water as an endogenous tracer instead of depending on vascular blood oxygenation level.This study aimed to assess the number of pulsed ASL blocks that were needed to provide accurate and reliable regional estimates of cerebral blood flow (CBF) changes when participants engaged in visually guided saccade and fixation task; evaluate the localization to cortical control saccade versus fixation; investigate the relationship between the sensitivity of ASL fMRI and the number of blocks; and compare the sensitivity of blood oxygen level-dependent (BOLD) fMRI and ASL fMRI.

Methods The experiment was a block-design paradigm consisting of two conditions: fixation and saccade. No response other than the eye movements of the participants was recorded during the scans. ASL and BOLD fMRI scans were conducted on all participants during the same session. The fMRI study consisted of two functional experiments: a CBF contrast was provided using the ASL sequence, and an optimized BOLD contrast was provided using the BOLD sequence.

Results From group analysis in all divided blocks of ASL sessions (4, 6, 8…… 14, 16, 18…….26, 28, 30), ASL yielded significant activation clusters in the visual cortex of the bilateral hemisphere from block 4. There was no false activation from block 4. No activation cluster was found by reversing analysis of block 2. Robust and consistent activation in the visual cortex was observed in each of the 14 divided blocks group analysis, and no activation was found in the eye field of the brain. The sensitivity of 4-block was found to be better than that of 8-block. More significant activation clusters of the visual cortex were found in BOLD than in ASL. No activation cluster of parietal eye field (PEF), frontal eye field (FEF) and supplementary eye field (SEF) was detected in ASL. The voxel size of the activation cluster increased with the increasing number of blocks, and the percent signal change in the activation cluster decreased with the escalating block number. The voxel size was positively correlated with the number of blocks (correlation coefficient = 0.98, $p < 0.0001$), and the percent signal change negatively correlated with the number of blocks (correlation coefficient = –0.90, $p < 0.0001$).

Conclusion The 4-block pulsed functional ASL (fASL) presents accurate and reliable activation, with minimal time-on-task effect and little adverse impact of time, in participants engaging in visually guided saccade and fixation tasks. Despite having lower sensitivity than BOLD fMRI, ASL can determine accurate activation location. Although the time-on-task effects affect the observation for the sensitivity of ASL over task time, it is suggested that ASL fMRI may provide a powerful method for pinpointing the time-on-task effect over a long period of time.

Key words: fASL; sensitivity; activation; blocks; saccade fixation

Submitted: 16 July 2024 Revised: 19 August 2024 Accepted: 2 September 2024

How to cite this article:
Li Q, Shen S, Ming L. Sensitivity of Functional Arterial Spin Labelling in Detecting Cerebral Blood Flow Changes. Br J Hosp Med. 2024. https://doi.org/10.12968/hmed.2024.0433

Introduction

Functional magnetic resonance imaging (fMRI) is commonly used to locate brain activation related to motor, sensory and cognitive activity. Direct measurement of neural activity stands as the ideal method for cognitive neuroscientists. For that, dynamic susceptibility contrast (DSC) magnetic resonance imaging (MRI) can be used for measuring changes in cerebral blood flow (CBF) as a consequence of neural activity, a method that makes DSC MRI the most direct approach to measuring neural activity. However, this method is invasive due to the utilization of exogenous contrast agents (Sourbron et al, 2009). An alternative to this method is blood oxygen level-dependent (BOLD) imaging fMRI, which reflects physiological processes dependent on CBF, cerebral blood volume (CBV) and cerebral metabolic rate of oxygen ($CMRO_2$) (Ogawa et al, 1993), a technique that has been widely adopted. It is worth noting that BOLD does not provide a direct measure of cerebral perfusion or CBF. Nevertheless, recent advances in MRI hardware and software have made completely non-invasive approach for direct measure increasingly possible.

One powerful technique currently being explored by the University of Michigan Functional MRI Laboratory is arterial spin labelling (ASL), a non-invasive MRI method that quantitatively measures CBF directly by magnetically tagging water protons in arterial blood as an endogenous tracer (Williams et al, 1992). Cerebral perfusion is responsible for the delivery of oxygen and nutrients from artery into the capillary bed of the brain parenchyma; in other words, CBF changes can be leveraged as a marker of brain function or brain activity (Kim, 1995), and it is tightly linked to neural activity. Similarly, the findings of one ASL study suggest that the linearity between CBF changes and neural activity may be stronger than the linearity between BOLD response and neural activity (Miller et al, 2001). Consequently, ASL measures can exhibit decreased inter-subject and inter-session variability as opposed to BOLD. The use of ASL to measure CBF changes can improve the interpretation of fMRI experiments.

ASL techniques can quantitatively measure cerebral perfusion by fitting a kinetic model to the difference between labelled images (tag images) and ones which are acquired without labelling (control images). A perfusion-weighted image is obtained from the successive pairwise subtraction of a tag image from a control image (Hernandez-Garcia et al, 2010). This subtraction process generates minimized drift effects in ASL perfusion contrast. In contrast, low-frequency drift effects in BOLD contrast result in poor sensitivity for detecting slow variations in neural activity (Weber et al, 2013). Hence, ASL is highly reproducible in intra-individual detection of neural activity over long task duration, making it well-suited for longitudinal studies.

ASL fMRI provides quantitative perfusion maps by using arterial water as an endogenous tracer instead of depending on vascular blood oxygenation level. Compared to the relatively venous-weighted BOLD method, ASL allows the weighting of the MRI signal by CBF so that absolute quantification of activation-related CBF is less sensitive to venous contamination than BOLD fMRI (Pollock et al, 2009).

ASL has a better potential in locating the sites of neural activity (Duong et al, 2001). A study by Raoult et al (2011) compared functional ASL (fASL) and BOLD fMRI for their accuracy of functionally locating hand motor area, concluding that the functional imaging protocols using ASL produce comparable results to a conventional BOLD protocol, with the additional advantages of better spatial specificity and quantification possibilities. Thus, ASL perfusion techniques offer direct and absolute quantification of brain activation associated with CBF. Additionally, fASL can detect brain activation more closely linked to neuronal activity, with higher spatial accuracy, while facing lesser inter-subject and inter-session variability than BOLD fMRI.

Despite their potential advantages, the use of ASL methods for fMRI studies has been rather limited, especially for cognitive functional studies. A significant limitation of ASL methods is their relatively low sensitivity as compared to BOLD methods (Hernandez-Garcia et al, 2010). Based on the same block-design paradigm and resolution, the experiment-determinate signal-to-noise ratio (SNR) of ASL perfusion fMRI is approximately lower than 50% that of BOLD fMRI (Liu and Brown, 2007). In an ASL perfusion fMRI study, due to T1 decay and transit time limitations, the tagged blood makes up a small fraction of the total blood flow to the tissue in the imaging plane, resulting in a perfusion signal for CBF that is only 1–5% of the mean tissue signal (Wong et al, 1999). In fASL experiments, the change in task-induced perfusion does not exceed the mid-level of the baseline perfusion signal, so the minimum signal changes caused by the inflow of the blood is probably 0.5% of the static tissue signal (Wang et al, 2008). Achieving an adequate SNR usually requires more data averaging (namely, more repeated acquisition) in order to obtain an image with adequate quality; approximately 40–100 ASL image pairs are typically required for measuring the CBF values at task-free resting state of the brain (Lim et al, 2008; Nöth et al, 2006; Wu et al, 2007). However, the existing literature presents only a small amount of ASL fMRI studies on motor tasks (Pimentel et al, 2013), visual sustained attention tasks (Hendriks et al, 2019), and visual and motor tasks performed simultaneously (Donahue et al, 2009)—these experiments adopted four blocks or equivalent acquisition sequences. The length of the acquisition sequences may depend on the studies about BOLD fMRI, because two- to four-block design paradigm has been successfully deployed in BOLD fMRI experiment (van Reekum et al, 2007). Since ASL fMRI and BOLD fMRI differ in physical properties and acquisition parameters, it is unfeasible to directly adopt and apply the blocks number from BOLD fMRI to ASL fMRI. Therefore, using the appropriate number of blocks in the ASL fMRI block design remains a pressing issue.

In this study, we selected a visually guided saccade task to investigate the sensitivity of fASL for two reasons. First, this task produces robust brain activation of a large-scale neurocognitive network. Anderson et al (1994) showed that positron emission tomography offers mapping evidence for examining cerebral function during saccadic and fixation performances. Through comparisons of saccade and fixation, significant activation was observed in visual cortex bilateral, parietal eye field located in the superior parietal lobule (SPL) and intraparietal sulcus, frontal eye field located in the precentral gyrus and superior frontal sulcus, and supplementary

eye field located in the upper medial wall of the frontal lobe. Similar anatomical landmarks of the human brain were found in the BOLD fMRI (Koyama et al, 2004). Second, these activated regions are separate in the brain, and ASL can detect each region with good sensitivity. These findings laid the basis for drawing a strong hypothesis that ASL holds promise for detecting brain activity by assessing saccade and fixation in these regions.

In the present study, we aimed to assess the number of pulsed ASL blocks that were needed to provide accurate and reliable regional estimates of CBF changes when participants engaged in visually guided saccade and fixation task; evaluate the localization to cortical control saccade versus fixation; investigate the relationship between the sensitivity of ASL fMRI and the number of blocks; and compare the sensitivity of BOLD and ASL fMRI. For this purpose, ASL blocks of task were split into the first 4, 6, 8, 10…..22, 24, 26, 28, 30, and activation cluster values were calculated from the data of 12 participants until a significantly reliable value was obtained. Four blocks were determined according to the minimum number of 2 blocks in typical BOLD fMRI (Evers et al, 2006; Rubia et al, 2001; Stevenson et al, 2007) and the scale of 1:2–SNR ASL/BOLD (Hernandez-Garcia et al, 2010).

Methods

Participants

Twelve physically healthy adults (7 males, 5 females) ranging in age from 20 to 66 years (33.8 ± 11.9) participated in the present study. The study was approved by the University of Reading Research Ethics Committee (Research Ethics Committee Project No. 11/20: Sensitivity of functional arterial spin labelling in detecting cerebral blood flow changes in the brain), and all participants gave written informed consent prior to participation. The study was carried out in compliance with the ethical principles stipulated in the Declaration of Helsinki.

MRI Task

The experiment was a block-design paradigm consisting of two conditions: fixation and saccade. In the fixation (baseline) block, a fixation cross was displayed at the center of the screen. In the saccade (activation) block, the participants were asked to visually track a dot as it randomly moved around the screen, in order to induce saccadic eye movements to activate the visual cortex and eye fields in the brain (Anderson et al, 1994; Koyama et al, 2004). All participants were presented with thirty 20-s periods of baseline alternating with thirty 20-s periods of activation for ASL. In an effort to control eye fatigue and habituation for maintaining the subjects' attention, 10 of the 12 subjects were instructed to close their eyes but stay still and open their eyes at three time points (320 s, 660 s, and 1040 s); after which, the participants were each given rest lasting 1 min. A total of 552 volumes (30 blocks and 3-min rest) alternating between tag and control were acquired for 10 subjects, resulting in a scan duration of 23 mins; a total of 480 alternating volumes (30 blocks) were acquired for two other subjects, with a scan duration of 20 mins. A block design with 8 cycles of alternating 20-s gaze and 20-s sweep tasks

was used for standard BOLD acquisition. Each functional scan collected a total of 128 volumes (8 blocks) with a total task scan time of 5 mins and 20-s. Stimuli were projected through an MRI-compatible visual display system (VisualSystem HD, NordicNeuroLab Inc., Bergen, Hordaland, Norway), which contains a built-in eye-tracking camera. No response other than the eye movements of the participants was obtained during the scans. Eye movements within the scanner were tracked using the Fovio eye-tracker system (Seeing Machines, Canberra, Australia).

Image Acquisition

ASL and BOLD fMRI scans were conducted on all participants during the same session, using a Siemens Trio 3T MRI scanner with a 12-channel coil (Siemens Healthcare, Erlangen, Nurnberg, Germany). The fMRI sessions included two functional experiments: one using an ASL sequence to provide a CBF contrast; and the other utilizing a BOLD sequence to provide an optimized BOLD contrast. The ASL acquisitions preceded the BOLD acquisitions across the subjects to ensure the completion of the ASL session. One participant failed to complete the BOLD acquisition because of unbearable fatigue. Consequently, the number of subjects who have completed BOLD acquisition is 11.

ASL Protocol

A method termed PICORE QUIPSS II with thin-slice TI1 periodic saturation (Q2TIPS) that falls under the category of pulsed ASL was employed (Villien et al, 2013). Setting TI1 at 700 ms enabled the inverted arterial spins to make their way to the imaging slab. During the interval between TI1 and TI1s which stood at 1600 ms (acting as the TI1 stop time), the acquisition of interleaved label and control images was executed at TI2 of 1700 ms with the aid of a gradient-echo (GRE) echo-planar imaging (EPI) readout module. The parameters for this acquisition encompassed a repetition time of 2.5 s, an echo time of 13 ms, and a flip angle of 90°. The imaging region comprised 18 adjoining axial slices having a thickness of 6.25 mm and an inter-slice separation of 1.25 mm. It is positioned parallel to the AC-PC axis, located between the top of the brain and the upper part of the cerebellum, in order to enclose the primary eye field. The imaging slices boasted a field of view (FOV) of 256×256 mm^2 and a matrix size of 64×64, thereby yielding a voxel resolution of $4 \times 4 \times 6.25$ mm^3. The slices were acquired in an interleaved manner.

BOLD Protocol

A standard BOLD protocol was harnessed to secure an optimized BOLD signal so as to enhance the comparability between BOLD and ASL measurements. Functional images were obtained via a multislice single-shot GRE-EPI sequence. The other imaging details were: repetition time (TR) equalled 2.5 s, echo time (TE) was 30 ms, flip angle was 90°, FOV measured 256×256 mm^2, and a matrix size was 64×64, giving rise to a voxel resolution of $4.0 \times 4.0 \times 6.25$ mm^3. The entire brain was encompassed by 25 successive axial slices having a thickness of 6.25 mm and positioned parallel to the anterior commissure-posterior commissure (AC-PC) axis. The slices were acquired in an interleaved way.

Additional Images

A calibration scan of single-shot EPI (M0) was carried out with a TR set at 5 s before the start of the experiment to compute the absolute CBF value. Before every functional scan, a main magnetic field (B0) map relying on a GRE sequence was obtained. This map had the same in-plane resolution as that to be employed in each functional acquisition yet with a distinct slice configuration: 30 slices in total, a slice thickness of 5.0 mm, and a 1.25 mm gap between the slices. Furthermore, a T1-weighted structural scan (with voxels measuring 1 × 1 × 1 mm) was also acquired for each subject for the sake of image registration. The parameters were as follows: an inversion time (TI) of 1100 ms, a TR of 2020 ms, a TE of 2.9 ms, 176 axial slices having a thickness of 1.0 mm, a flip angle of 9°, a FOV of 250 × 250 mm^2, and a matrix size of 256 × 246.

Image Analysis

Image analysis was conducted using FEAT Version 6.00 (FMRIB's Expert Analysis Tool) from FSL (Oxford University, Oxford, UK). Pre-statistics processing on all datasets with FSL software package (http://www.fmrib.ox.ac.uk/fsl/) included non-brain removal with brain extraction tool (BET) (Alhamud et al, 2015), motion correction via MCFLIRT (Marami et al, 2016), high-pass temporal filtering at an 80-ms cutoff, grand-mean intensity normalization of the 4D dataset by a single factor, EPI-distortion correction using FUGUE (FMRIB's Utility for Geometrically Unwarping EPIs, http://www.fmrib.ox.ac.uk/fsl/) (Yang et al, 2024), and ICA-based exploratory data analysis with MELODIC (http://www.fmrib.ox.ac.uk/fsl/) (Beckmann and Smith, 2005) to check for artifacts or activation. For activation detection in ASL and BOLD fMRI, lower ASL sensitivity compared to that of BOLD and a reasonable spatial smoothing estimate, which was 2–3 times the voxel size, were considered, and a Gaussian kernel of full width at half maximum (FWHM) 12 mm for ASL and 8 mm for BOLD was used (Candemir, 2023). Additionally, to compare their sensitivities with the same parameter, 8-mm Gaussian spatial smoothing was applied to ASL fMRI.

Time-series statistical analysis was then conducted in accordance with a general linear model (GLM) approach by employing FMRIB's enhanced linear model (FILM) along with local autocorrelation correction via pre-whitening (Olszowy et al, 2019) to spot the task-activated voxels in connection with each contrast. Within this statistical analysis procedure, GLM is fit for the ASL protocol and can boost the statistical potency. This is because the CBF alterations which ASL might measure have a robust linear connection with neural activities. For the BOLD protocol, a single task-related explanatory variable (EV1) was defined by convolving the block paradigm with a double gamma function (phase of 0 s) that models the hemodynamic response function (Boynton et al, 1996). For the ASL protocol, a GLM framework encompassing a complete perfusion signal model was also utilized. Task-related EV2 models the BOLD signal, and an additional ASL-related explanatory variable (EV1) models the switching between control and tag volumes when there is no stimulation present. Subsequently, the interaction between the control-tag alternation (EV1) and the saccade task (EV2) variables was taken into

account by multiplying EV1 by EV2 to model the activation component of the perfusion-weighted signal (EV3). It is close to zero during fixation and ascends in amplitude during a saccade.

The data was fitted with the GLM defined by the EV, and the parameter estimates relevant to each EV were ascertained. Subsequently, the contrast of ASL was defined as EV3 in comparison to the baseline. Then, a *t*-test was implemented, yielding a Z (Gaussianized *t*/F) statistic map for the ASL contrast. A dependable threshold was selected for both protocols. As a result, the Z maps were thresholded using a clustering process where each cluster was determined by a voxel Z exceeding 2.3 and a (corrected) cluster significance threshold of $p = 0.05$ (Salli et al, 2001).

After the statistical analysis for each participant's data was completed, as per standard step, spatial normalization was carried out. To conduct inter-subject comparisons and group analyses for both ASL and BOLD data in half of the participants, the registration of the functional images to the corresponding individual T1-weighted structural images and the $1 \times 1 \times 1$ mm^3, Montreal Neurological Institute (MNI) standard brain (Collins et al, 1994) was accomplished using FMRIB's Linear Image Registration Tool (FLIRT) (Jenkinson and Smith, 2001), with 6 and 12 degrees of freedom, respectively. In the case of the other half, the registration of the functional images to the structural image was performed by employing the boundary-based registration (BBR) cost function along with field maps. For all participants, except for one (where the registration between the subject's structural image and standard space using nonlinear methods failed), we further applied nonlinear registration (Dohmatob et al, 2018) between the subject's structural image and standard space to achieve better registration for the group analysis. For each contrast, higher-level group analyses were executed using FMRIB's Local Analysis of Mixed Effects, which is a part of FSL (Olszowy et al, 2019; Chen et al, 2019). This tool modelled and estimated the random effects and experimental conditions of the measured inter-session mixed-effects variance.

Data Analysis

The ASL blocks of the task were split into the first 4, 6, 8…… 14, 16, 18…… 26, 28, 30 for group analysis of 12 participants. Four blocks were determined according to the minimal number of 2 blocks in typical BOLD fMRI (Evers et al, 2006; Rubia et al, 2001; Stevenson et al, 2007) and the scale of 1:2–SNR ASL/BOLD (Hernandez-Garcia et al, 2010). Then, the BOLD blocks were split in half to obtain 4- and 8-block data for 11 participants, due to a consensus that the 4-block design is likely to be reasonable and reliable in BOLD fMRI experiments (van Reekum et al, 2007). The analysis of brain activation using ASL CBF contrast (ASL) and BOLD contrast (BOLD) were considered for assessment of the number of pulsed ASL blocks that were needed to detect activation, evaluation of localization of brain activation in the saccade versus fixation comparison, and investigation of the relationship between the sensitivity of ASL fMRI and the number of blocks. The two contrasts were obtained by using cluster threshold (a voxel $Z > 2.3$ and a corrected

cluster significance threshold $p = 0.05$). Differences in measurement data between ASL and BOLD were determined by paired sample *t*-test.

CBF Changes of Saccade Versus Fixation Condition

The regional CBF change of activation versus baseline was quantified by calculating the percentage signal change in the locator from fixation to saccade condition. This quantitative analysis provides an evaluation of brain activity upon stimulation. There are a couple of locators for calculating the percent signal change:

(1) The center of gravity (COG) for the activation cluster. This location is defined as a weighted average of the coordinates by the intensities in the activation cluster. The COG can sufficiently determine the location of the activation regardless of the activation cluster size (Pimentel et al, 2013).

(2) The activation clusters. These are hypothesized activated regions containing visual cortex, parietal eye field (PEF), frontal eye field (FEF), and supplementary eye field (SEF). COG and activation clusters as localizers were used to detect signal change across the different ASL block groups. The percent signal change in COG and activation clusters was generated using Featquery (Prodanov, 2011) in FSL.

Results

Accuracy and Reliability of ASL Activation

In the group analysis, the ASL sessions were divided into different blocks: 4, 6, 8…… 14, 16, 18…….26, 28, 30. Examples for group analysis of 4 blocks, 10 blocks, 16 blocks, 22 blocks and 30 blocks are shown in Fig. 1. ASL produced significant activation clusters in the visual cortex of both hemispheres starting from block 4. Meanwhile, there was no false activation from block 4. No activation cluster was found by reversing analysis of block 2. These findings suggest ASL session of at least 4 blocks was required to detect the brain activation in response to the visually guided saccade versus fixation. Robust and consistent activation in the visual cortex was observed in each of the 14 divided blocks group analysis, and no activation was found in eye field of brain, indicating that visual cortex has strong activation during saccadic versus fixation task.

BOLD Activation of Saccade Versus Fixation Condition

The activation clusters of 4 blocks and 8 blocks BOLD session are shown in Fig. 2. A comparison of both BOLD sessions revealed that there were five particularly significant activation clusters in bilateral visual cortex, bilateral SPL, bilateral precentral gyrus/superior frontal sulcus and bilateral medical frontal gyrus in the 4-block session, but certain expected activations of SPL, FEF and SEF were not detected in the 8-block session. The results that the sensitivity of the 4-block design was visualized better than the 8-block one is contrary to the generalization that the sensitivity can be improved by performing more repeated acquisition sequences. This discrepancy may be caused by systematic effects of fatigue or habituation.

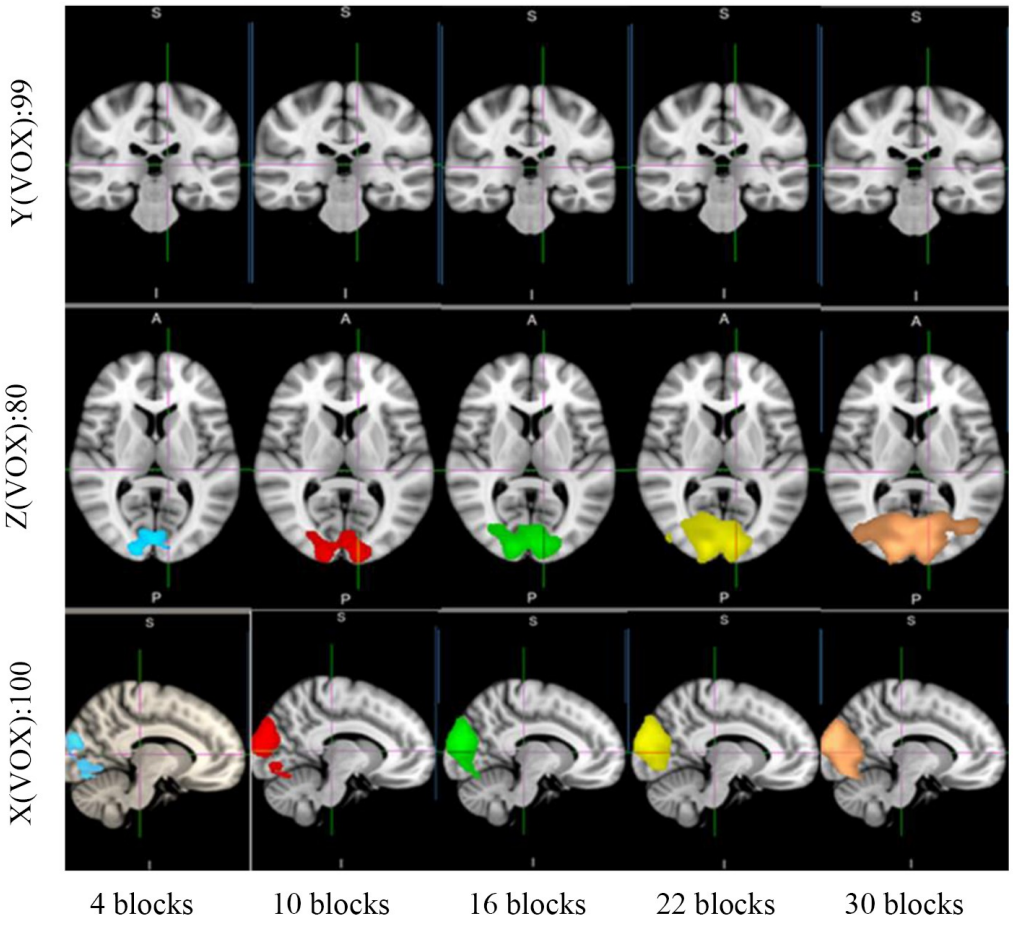

Fig. 1. Arterial spin labelling (ASL) activation associated with saccade versus fixation (n = 12). Examples of Z maps of activation obtained from group analysis of 4-block (blue), 10-block (red), 16-block (green), 22-block (yellow), and 30-block (copper) ASL session, superimposed on the standard Montreal Neurological Institute (MNI) brain templates are shown. Each image is indicated with a voxel coordinate in the MNI space.

Comparison of Activation in ASL and BOLD Sessions

The results of group analysis of 4-block ASL and BOLD sessions are shown in Fig. 3. More significant activation clusters of visual cortex were found in BOLD session than in ASL session, suggesting that the sensitivity of ASL is lower than that of BOLD. Additionally, no activation cluster of PEF, FEF and SEF was detected in ASL session. The result indicates that the activation of eye field is weaker than that of visual cortex, offering an explanation of the unsuccessful activation detection in ASL session due to lower sensitivity.

The Relationship of Activation in the ASL with the Number of Blocks

The relationship among the voxel size of activation cluster, percent signal change of COG and activation cluster in ASL different divided blocks group with the number of blocks was statistically analyzed. The mean and standard deviation of voxel size of activation cluster, percent signal change of COG and activation cluster across the ASL divided blocks group in the visual cortex are shown in Ta-

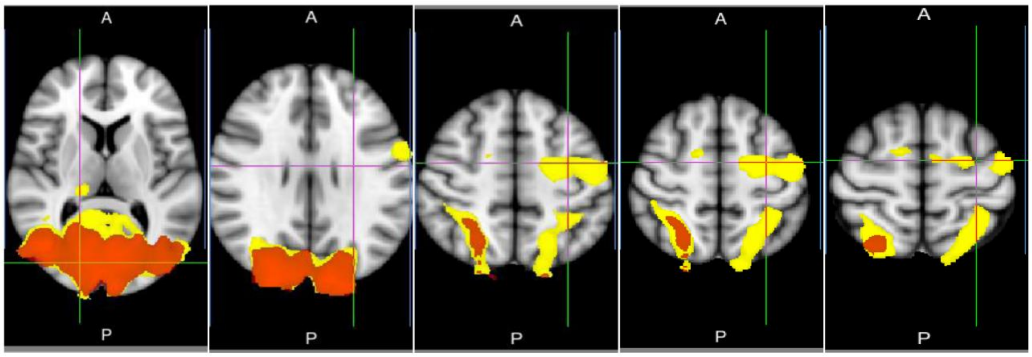

Fig. 2. Blood oxygen level-dependent (BOLD) activation associated with saccade versus fixation (n = 11). Activation was detected by group analysis of 4-block (yellow) and 8-block (red) BOLD sessions. Both overlapping Z maps were displayed in transverse projection, superimposed on the standard MNI brain templates. Each image is indicated with a Z coordinate (mm) in the MNI space.

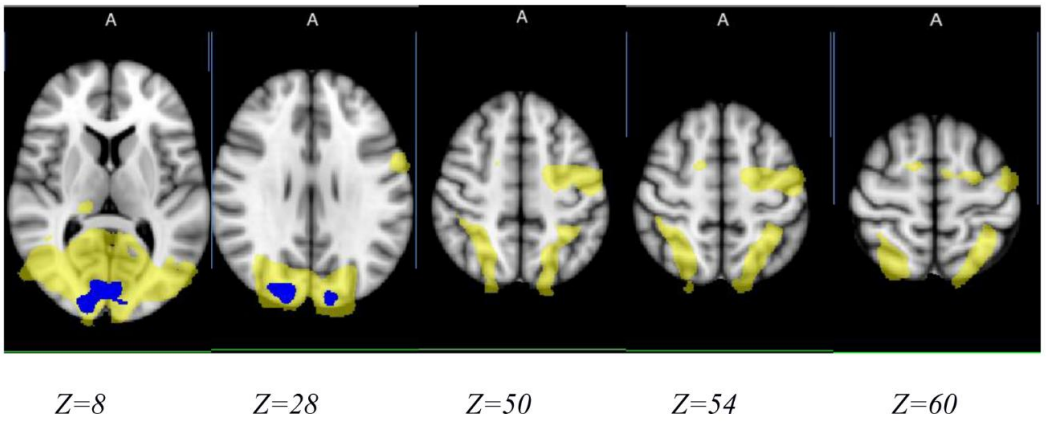

Fig. 3. ASL and BOLD activations associated with saccade versus fixation (n = 11). Saccade-related activation was detected by group analysis of 4-block BOLD (yellow) and ASL (blue) sessions. Both overlapping Z maps are displayed in transverse projection, superimposed on the standard MNI brain templates. Each image is indicated with a Z coordinate (mm) in the MNI space. A full width at half maximum (FWHM) of 12 mm for ASL and 8 mm for BOLD was used during spatial smoothing.

ble 1. Since activation cluster was the only cluster survived in the visual cortex of each ASL divided blocks group, the activation in visual cortex became the sole subject of analysis in this study.

Fig. 4 shows the voxel size of activation cluster increases with increasing number of blocks, whereas Fig. 5 shows the percent signal change of activation cluster in the visual cortex decreases with the escalating blocks number. Correlation analyses were performed between voxel size or percent signal change of activation cluster in visual cortex and the number of blocks, showing that the number of blocks is positively correlated with the voxel size (correlation coefficient = 0.98, $p < 0.0001$) and negatively correlated with the percent signal change (correlation coefficient =

Table 1. Average and standard deviation of voxel size of activation cluster, percent signal change of COG and activation cluster across the divided blocks group (n = 12).

Acti activation cluster	Voxel size	PSC of COG (%; mean ± SD)	PSC of cluster (%; mean ± SD)
Visual cortex	64,021.86 ± 30,326.57	0.0371921 ± 0.00573921	0.0330221 ± 0.00582056

Abbreviations: COG, center of gravity; PSC, percent signal change.

–0.90, $p < 0.0001$). Here, the voxel size of activation cluster is corresponding to SNR. The results are consistent with the SNR of ASL becoming higher with longer acquisition sequences. On the contrary, regional CBF changes represented by the percent signal change declined with more repeated blocks. The combination of BOLD and ASL activation associated with saccade versus fixation generates the deduction that repeated saccade stimulus may weaken regional CBF change as a response to activation.

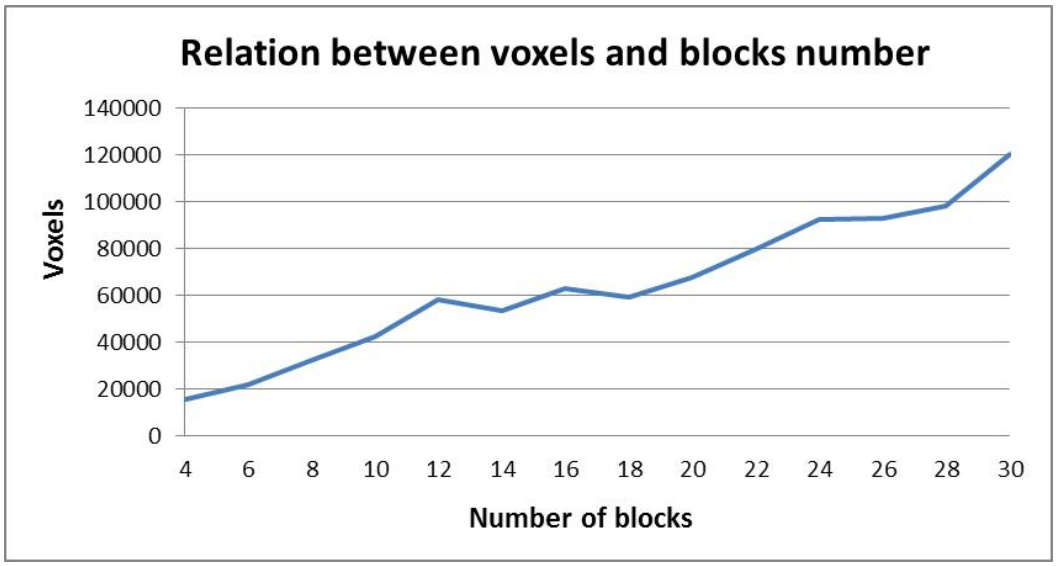

Fig. 4. The relationship between voxel size of activation cluster in visual cortex and the number of blocks.

The Functional Localization of Brain Activation

Examples of Z map of ASLuncorr (uncorrected voxel $p < 0.05$) from 4-, 16- and 30-block ASL group analysis are shown in Fig. 6. With the less demanding thresholding procedure (voxel $p < 0.05$), we could detect significant activation clusters in left SPL and left precentral gyrus that belong to parietal and frontal eye field regions. Through the visualized observation, activation clusters in the SPL and precentral gyrus are mainly distributed in left brain, and there is no apparent difference of the activation clusters in left SPL and left precentral gyrus across 4-, 16- and 30-block ASLuncorr.

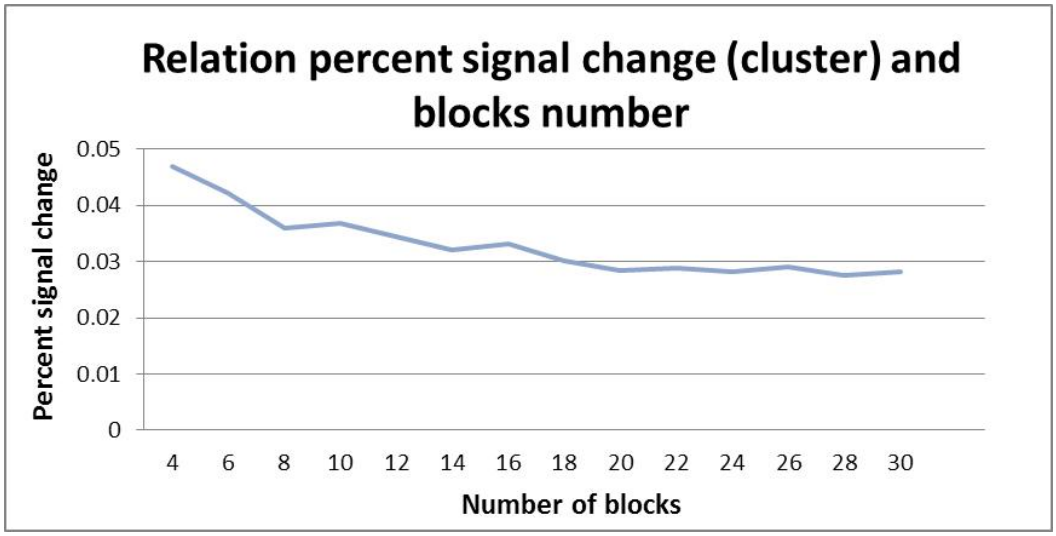

Fig. 5. The relationship between percent signal change of activation cluster in visual cortex and the number of blocks.

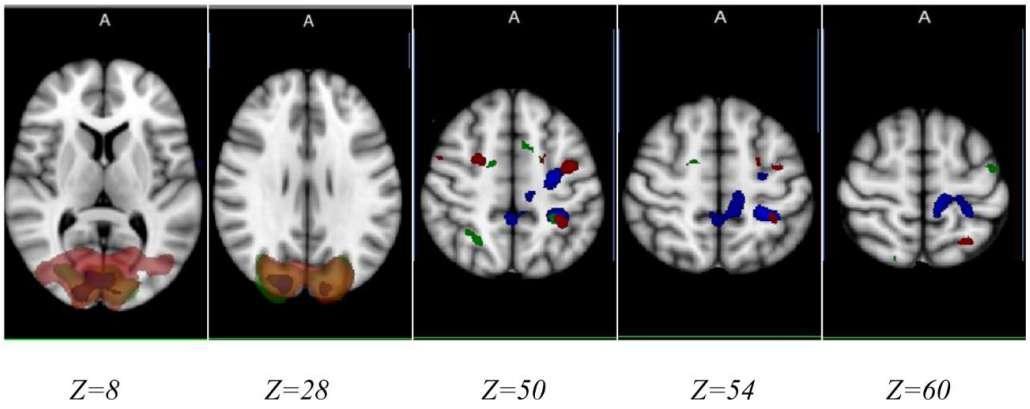

Fig. 6. Activation corresponding to ASLuncorr. Saccade-related activation was detected by group analysis of 4 blocks (blue), 16 blocks (green) and 30 blocks (red) ASL (n = 12). Three overlapping Z maps are displayed in transverse projection, processed with less demanding thresholds (voxel $p < 0.05$), and superimposed on the standard MNI brain template. Each image is indicated with the Z coordinate (mm) in the MNI space.

The Relationship of Block Number with Voxel Size and Activation Cluster

The relationship between voxel size of activation cluster in the left SPL or left precentral gyrus and the number of blocks is shown in Fig. 7, which depicts that the voxel size of activation clusters fluctuates with the number of blocks. The relationship between percent signal change of activation cluster in left SPL or left precentral gyrus and blocks number is shown in Fig. 8, and the relationship between percent signal change of COG in left SPL and left precentral gyrus and blocks number is shown in Fig. 9. Both Figs. 8,9 show that the percent signal change of activation clusters and COG decreases with the rising blocks number.

Correlation analyses between voxel size or percent signal change of COG or activation cluster in left SPL or left precentral gyrus and the number of blocks were

also performed. The results show that there is no correlation between voxel size and blocks number (for cluster 2, $p = 0.48$; for cluster 3, $p = 0.055$), whereas the percent signal change of COG is negatively correlated with the number of blocks (for cluster 2, correlation coefficient = –0.81, $p < 0.0001$; for cluster 3, correlation coefficient = –0.80, $p < 0.0001$); the correlation between percent signal change of activation clusters and blocks number is also shown to be negative (for cluster 2, correlation coefficient = –0.81, $p < 0.0001$; for cluster 3, correlation coefficient = –0.83, $p < 0.0001$). The results also show that activation of eye field weakened with increasing number of blocks, striking a similar note in the context of activation of visual cortex. Theoretically, performing more repeated acquisition sequences (leading to averaging of more tag–control image pairs) could improve the sensitivity. However, there is a negative association between activation of regions of interest (ROIs) and time; meanwhile, the same relationship is also presented in BOLD. This finding may be accounted for by the time-on-task effects.

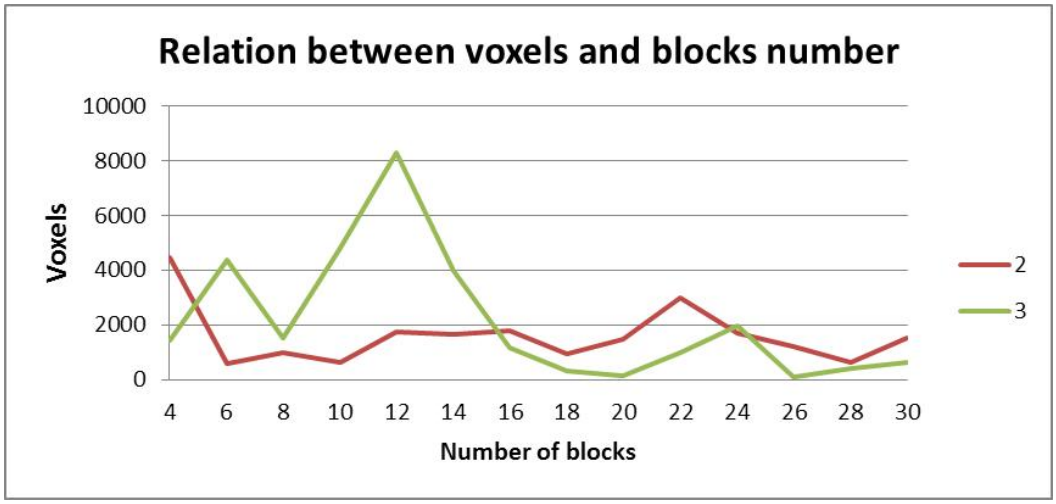

Fig. 7. The relationship between voxel size of activation cluster in left superior parietal lobule (SPL) or left precentral gyrus and the number of blocks. In the graph, curve 2 represents the left SPL whereas curve 3 denotes the left precentral gyrus.

Comparison of Activation in the ASL Divided Blocks Group

The mean and standard deviation values of voxel size of activation cluster, percent signal change of COG and activation cluster calculated from the 14-block ASL group for two activation clusters are displayed in Table 2. The two activation clusters were found in left SPL (activation cluster 2) and left precentral gyrus (activation cluster 3). The two activation clusters were found in Z map of ASLuncorr across ASL divided blocks group. No sufficiently significant voxel size differences exist in cluster 2 versus cluster 3 (t [1, 26] = 0.80, $p = 0.4286$). There were no differences in percent signal change in COG between clusters 2 and 3 (t [1, 26] = 0.85, $p = 0.4031$). Percent signal change of cluster 2 was statistically different from that of cluster 3 (t [1, 26] = 1.33, $p = 0.1940$).

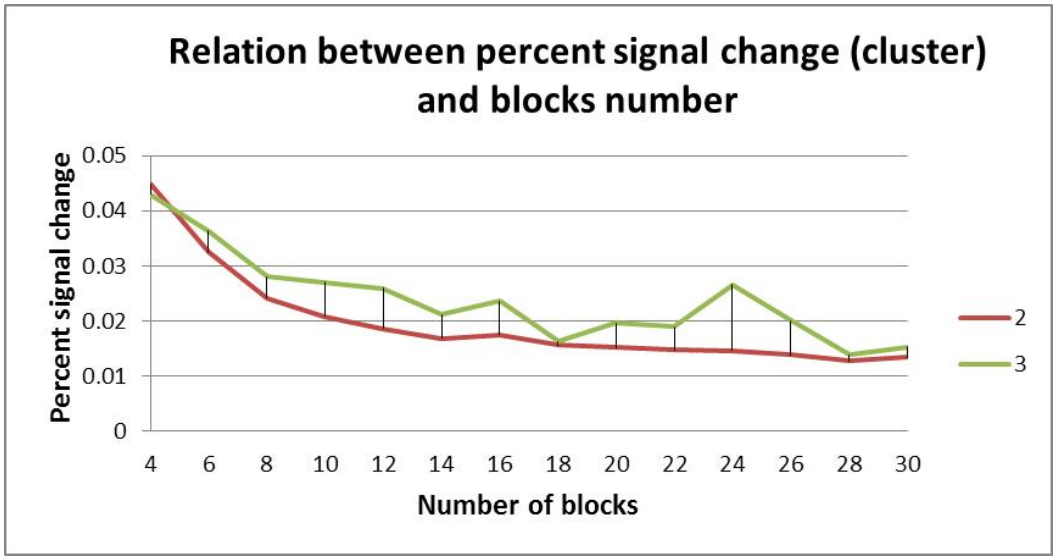

Fig. 8. The relationship between percent signal change of activation cluster in visual cortex and the number of blocks. In the graph, curve 2 represents the left SPL whereas curve 3 denotes the left precentral gyrus.

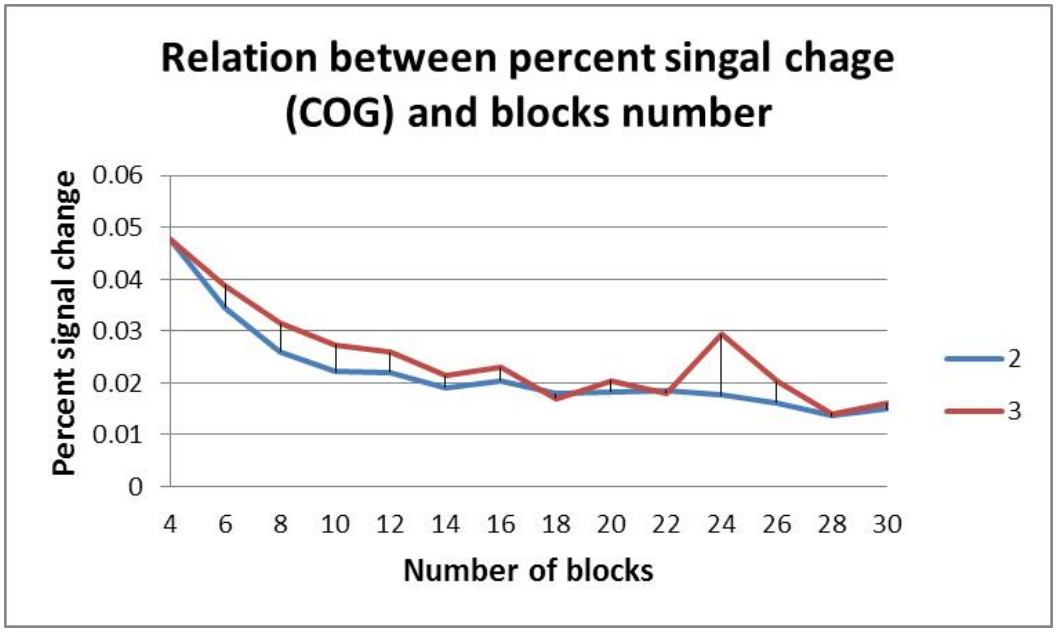

Fig. 9. The relationship between percent signal change of COG in left SPL or left precentral gyrus and the number of blocks. In the graph, curve 2 represents the left SPL whereas curve 3 denotes the left precentral gyrus. Abbreviation: COG, center of gravity.

Discussion

This study presented that 4-block pulsed ASL can reflect accurate and reliable regional CBF changes when participants engaged in visually guided saccade task. The essential data were collected within 2 min 40 s—a very rapid image acquisition process to minimize adverse impacts like head motion and attention fatigue. The results of this study provide guidance for developing block-design paradigm

Table 2. Average and standard deviation of voxel size of activation cluster, percent signal change of COG and activation cluster across the divided blocks group.

Activation cluster	Voxel size	PSC of COG (%; mean ± SD)	PSC of cluster (%; mean ± SD)
2	1591.43 ± 1038.824	0.0221107 ± 0.00902746	0.0196614 ± 0.00897168
3	2147.71 ± 2370.712	0.0239771 ± 0.00940074	0.0239771 ± 0.00813457

Note: Activation cluster 2 represents the left SPL whereas cluster 3 denotes the left precentral gyrus.
Abbreviations: COG, center of gravity; PSC, percent signal change.

of ASL fMRI studies. So far, only a small amount of ASL fMRI studies have deployed block-design paradigm during task-performing. For example, in Pimentel et al.' study (2013), 4-block ASL session (the period of each task was 30 s, TR = 2.25 s) detected significant activation in hand motor area of brain during motor activation task. Raoult et al.'s experiment (2011) employed 7-block ASL session (each of the condition lasted 30 s, TR = 3 s) in which the participants undertook a right hand motor task, which yielded motor activation mapping results depicting spatial accuracy. Regardless of the fact that these studies did not focus on assessing the number of blocks required to provide accurate and reliable activation when participants performed in tasks, these block-design paradigms are worth-while reference for these experiments.

The involvement of the visual cortex, FEF, PEF, and SEF associated with saccade versus fixation from 4-block BOLD was in accordance with previous neuroimaging studies (Anderson et al, 1994; Koyama et al, 2004). Activation regions of BOLD in our study were in consistence with the hypothesized task-related activation regions, signifying the successful completion of the tasks executed in this experiment.

Furthermore, in order to investigate the relationship between the sensitivity of ASL fMRI and the number of blocks, and compare the sensitivity of ASL with BOLD, we firstly obtained the activation clusters by two contrasts (BOLDuncorr, ASLuncorr), which survived more activation clusters using the less demanding threshold procedure. Secondly, the functional localization of brain activation stimulated by saccade versus fixation was used for ROIs selection. Our result in the 4-block BOLD session is consistent with previous neuroimaging studies (Anderson et al, 1994; Koyama et al, 2004). Thus, combining the Z map of ASLuncorr and BOLDuncorr divided blocks group with anatomical landmarks reference, ROIs were selected from the visual cortex and two main eye fields that are located in left SPL and left precentral gyrus, because the activation clusters in the three ROIs had more voxel size across divided blocks. Then, across the divided blocks, three activation clusters were selected on grounds of being in the corresponding three ROIs and having higher cluster index ranking from ASLuncorr and BOLDuncorr. These ROIs were specified from Harvard–Oxford Cortical Structural Atlases, packaged within the FSL. The activation clusters were extracted using fslmaths in FSL. Finally, we compared the voxel size of activation cluster, percent signal change of COG and activation cluster obtained for each ASL and BOLD divided blocks group in the three ROIs.

Comparison of Different Activation Clusters in ROIs

Attention to a regular and repeated presentation of same task would often be subject to progressive waning, thus generating "time-on-task effect" or "cognitive fatigue" or "habituation" (Mackworth, 1968). Liu et al (2022) investigated the network of time-on-task effect using ASL perfusion fMRI. In their study, a psychomotor vigilance test that tested motor reaction time to visual stimuli activated attention network, particularly the right lateralized fronto-parietal network. As previous suggested by Büchel et al (1998), the functional anatomical areas of attention to visual motion included not only extrastriate cortex areas but also parietal and prefrontal cortex. Furthermore, the detailed attention-related landmarks have been depicted, activation of extrastriate cortex included V3a bilaterally and V5 complex (V3a and V5 were defined by Talairach & Tournoux) (Nowinski et al, 1997); activation of parietal cortex involved the superior parietal gyrus bilaterally and extended along the intraparietal sulcus to supramarginal gyrus; activation of right prefrontal cortex was located in a medial part of the inferior frontal sulcus. Thus, spatial attention and eye movement processes shared not only inseparable mechanisms but also indivisible functional anatomical areas (Cabeza and Nyberg, 2000; Corbetta et al, 1998; Lewin et al, 1996).

Comparison of Activation in the Different ASL Divided Blocks Group

The purpose of this study was to investigate the relationship between the sensitivity of ASL fMRI and the length of acquisition sequences. Hence, despite the scheduled breaks, the tasks of this study were designed with more repeated stimulus and extended testing time, which inevitably contributed to the time-on-task effects in this study. These effects, which generated attention decrement and habituation, resulted in decreased regional CBF in visual, parietal and prefrontal cortex, especially right parietal and frontal eye field; then, the original activation of visual cortex and parietal and frontal eye field dwindled with performing saccade and fixation. Koyama et al (2004) had attempted to locate cortical eye fields associated with saccade using BOLD. Considering the attention impact on activation of saccade, the total time taken to complete the task was cut short to 240–288 s. Therefore, the finding that the activation of ROIs decreased with increasing number of blocks—particularly in the right parietal and frontal eye field—needs to be subjected to reasonable and cautious interpretation. Although the time-on-task effects had an impact on achieving the purpose of this study, this finding lends a counterargument that ASL method is capable of measuring varying brain activity such as attention deficits in a gradual manner.

Compare the Sensitivity of ASL fMRI and BOLD

Based on the 8-mm Gaussian spatial smoothing, we compared the percent signal change in the 8-block ASL and BOLD. The sum of percent signal change of the three activation clusters in 8-block BOLD session is 1.60%, whereas the value of 8-block ASL session is 0.12%. The percent signal change in BOLD is approximately tenfold of the value in ASL. This quantitative comparison demonstrated that the sensitivity of ASL fMRI is extremely lower than BOLD, consistent with

previous studies (Zou et al, 2015; Wong et al, 1999). The minimum task-induced signal changes may be 0.5% of the static tissue signal (Wang et al, 2008), whereas the value in this study is much lower than 0.5%. There are two possible reasons resulting in this disparity: under-detection of signal changes, especially in study consisting of few subjects, and unsuitable task administered. The adverse impact of unsuitable task has been illustrated previously (Mackworth, 1968).

Limitations of this Study

Based on the variability in the percent signal change from the subject-by-subject in ASL 4 blocks, the number of subjects was determined by power calculations G* power tool (University of Dusseldorf, Germany). Because no activation clusters of SPL and precentral gyrus were detected in 4-block ASL session, these regions were considered in the process of calculating sample size. The sample size computed based on the two regions, with a raised signal detection power of 80% and level of significance of 0.05, was estimated to exceed 12 subjects, the number used in the current study. To detect a 0.42% signal change in the SPL, the experiment needs 36 subjects; to obtain a 0.44% signal change in the precentral gyrus, 32 subjects are needed. Two prior studies have examined the task-correlated signal change. A study by Weber et al (2013) seen that significant signal change was found when a few subjects undertook tasks. In the present study, the sample size was estimated based on the means and variances of the sample, which was unknown at the start of the study. This highlights that sample sizes depend on the task by a large extent. Therefore, the proposed number of subjects is subject to change with the task administered.

To demonstrate further the time-on-task effects presented in this study, we analyzed the blocks preceding the 4-block session to assess whether the time-on-task effects affect activation related to visual stimulation in early task. Besides, Nordic-NeuroLab eye tracking hardware was used to inspect visual attention.

Conclusion

In conclusion, the 4-block pulsed fASL presents accurate and reliable activation, with few time-on-task effect and little adverse impact of time, in participants engaging in visually guided saccade and fixation task. Despite the lower sensitivity compared to BOLD fMRI, ASL can accurately locate the activation. Although the time-on-task effects have an influence on the sensitivity of ASL over task time, ASL fMRI is still a potentially powerful imaging strategy for delineating the time-on-task effect over a long time. Further research involving larger samples performing the task, with minimal time-on-task effects, is warranted to investigate the sensitivity of fASL in detecting CBF changes.

Key Points

- 4-block pulsed ASL can offer an accurate and reliable view of the regional cerebral blood flow (CBF) changes.
- The visual cortex, frontal eye field (FEF), parietal eye field (PEF), and supplementary eye field (SEF) are associated with saccade versus fixation.
- The activation of regions of interest decreases with increasing number of blocks.
- The voxel size of activation cluster increases with increasing number of blocks.
- The sensitivity of ASL fMRI is extremely lower than that of BOLD fMRI.

Availability of Data and Materials

All data included in this study are available upon request by contact with the corresponding author.

Author Contributions

QL and SS designed the study. SS collected the data. LM analyzed the data. QL drafted the manuscript. All authors contributed to the important editorial changes in the manuscript. All authors read and approved the final manuscript. All authors have participated sufficiently in the work and agreed to be accountable for all aspects of the work.

Ethics Approval and Consent to Participate

This study is being carried out in compliance with the ethical principles of the Declaration of Helsinki, and approved by the University of Reading Research Ethics Committee (Research Ethics Committee Project No. 11/20: Sensitivity of functional arterial spin labelling in detecting cerebral blood flow changes in the brain). Signed written informed consents were obtained from the patients and/or guardians prior to participation.

Acknowledgement

We thank Dr. David Field for providing the task template, Laura Inman for MRI data collection, and the Centre for Integrative Neuroscience and Neurodynamic (CINN) for IT support.

Funding

This study is supported by The Yangtze River Shipping Administration of Science and Technology Projects (202010017).

Conflict of Interest

The authors declare no conflict of interest.

References

Alhamud A, Taylor PA, Laughton B, van der Kouwe AJ, Meintjes EM. Motion artifact reduction in pediatric diffusion tensor imaging using fast prospective correction. Journal of Magnetic Resonance Imaging. 2015; 41: 1353–1364. https://doi.org/10.1002/jmri.24678

Anderson TJ, Jenkins IH, Brooks DJ, Hawken MB, Frackowiak RS, Kennard C. Cortical control of saccades and fixation in man. A PET study. Brain. 1994; 117: 1073–1084. https://doi.org/10.1093/brain/117.5.1073

Beckmann CF, Smith SM. Tensorial extensions of independent component analysis for multisubject FMRI analysis. NeuroImage. 2005; 25: 294–311. https://doi.org/10.1016/j.neuroimage.2004.10.043

Boynton GM, Engel SA, Glover GH, Heeger DJ. Linear systems analysis of functional magnetic resonance imaging in human V1. The Journal of Neuroscience. 1996; 16: 4207–4221. https://doi.org/10.1523/JNEUROSCI.16-13-04207.1996

Büchel C, Josephs O, Rees G, Turner R, Frith CD, Friston KJ. The functional anatomy of attention to visual motion. A functional MRI study. Brain. 1998; 121: 1281–1294. https://doi.org/10.1093/brain/121.7.1281

Cabeza R, Nyberg L. Imaging cognition II: An empirical review of 275 PET and fMRI studies. Journal of Cognitive Neuroscience. 2000; 12: 1–47. https://doi.org/10.1162/08989290051137585

Candemir C. Spatial Smoothing Effect on Group-Level Functional Connectivity during Resting and Task-Based fMRI. Sensors (Basel, Switzerland). 2023; 23: 5866. https://doi.org/10.3390/s23135866

Chen G, Bürkner PC, Taylor PA, Li Z, Yin L, Glen DR, et al. An integrative Bayesian approach to matrix-based analysis in neuroimaging. Human Brain Mapping. 2019; 40: 4072–4090. https://doi.org/10.1002/hbm.24686

Collins DL, Neelin P, Peters TM, Evans AC. Automatic 3D intersubject registration of MR volumetric data in standardized Talairach space. Journal of Computer Assisted Tomography. 1994; 18: 192–205.

Corbetta M, Akbudak E, Conturo TE, Snyder AZ, Ollinger JM, Drury HA, et al. A common network of functional areas for attention and eye movements. Neuron. 1998; 21: 761–773. https://doi.org/10.1016/s0896-6273(00)80593-0

Dohmatob E, Varoquaux G, Thirion B. Inter-subject Registration of Functional Images: Do We Need Anatomical Images? Frontiers in Neuroscience. 2018; 12: 64. https://doi.org/10.3389/fnins.2018.00064

Donahue MJ, Blicher JU, Østergaard L, Feinberg DA, MacIntosh BJ, Miller KL, et al. Cerebral blood flow, blood volume, and oxygen metabolism dynamics in human visual and motor cortex as measured by whole-brain multi-modal magnetic resonance imaging. Journal of Cerebral Blood Flow and Metabolism. 2009; 29: 1856–1866. https://doi.org/10.1038/jcbfm.2009.107

Duong TQ, Kim DS, Uğurbil K, Kim SG. Localized cerebral blood flow response at submillimeter columnar resolution. Proceedings of the National Academy of Sciences of the United States of America. 2001; 98: 10904–10909. https://doi.org/10.1073/pnas.191101098

Evers EAT, van der Veen FM, van Deursen JA, Schmitt JAJ, Deutz NEP, Jolles J. The effect of acute tryptophan depletion on the BOLD response during performance monitoring and response inhibition in healthy male volunteers. Psychopharmacology. 2006; 187: 200–208. https://doi.org/10.1007/s00213-006-0411-6

Hendriks AD, van der Kemp WJM, Luijten PR, Petridou N, Klomp DWJ. SNR optimized 31 P functional MRS to detect mitochondrial and extracellular pH change during visual stimulation. NMR in Biomedicine. 2019; 32: e4137. https://doi.org/10.1002/nbm.4137

Hernandez-Garcia L, Jahanian H, Rowe DB. Quantitative analysis of arterial spin labeling FMRI data using a general linear model. Magnetic Resonance Imaging. 2010; 28: 919–927. https://doi.org/10.1016/j.mri.2010.03.035

Jenkinson M, Smith S. A global optimisation method for robust affine registration of brain images. Medical Image Analysis. 2001; 5: 143–156. https://doi.org/10.1016/s1361-8415(01)00036-6

Kim SG. Quantification of relative cerebral blood flow change by flow-sensitive alternating inversion recovery (FAIR) technique: application to functional mapping. Magnetic Resonance in Medicine. 1995; 34: 293–301. https://doi.org/10.1002/mrm.1910340303

Koyama M, Hasegawa I, Osada T, Adachi Y, Nakahara K, Miyashita Y. Functional magnetic resonance imaging of macaque monkeys performing visually guided saccade tasks: comparison of cortical eye fields with humans. Neuron. 2004; 41: 795–807. https://doi.org/10.1016/s0896-6273(04)00047-9

Lewin JS, Friedman L, Wu D, Miller DA, Thompson LA, Klein SK, et al. Cortical localization of human sustained attention: detection with functional MR using a visual vigilance paradigm. Journal of Computer Assisted Tomography. 1996; 20: 695–701. https://doi.org/10.1097/00004728-199609000-00002

Lim YM, Cho YW, Shamim S, Solomon J, Birn R, Luh WM, et al. Usefulness of pulsed arterial spin labeling MR imaging in mesial temporal lobe epilepsy. Epilepsy Research. 2008; 82: 183–189. https://doi.org/10.1016/j.eplepsyres.2008.08.001

Liu TT, Brown GG. Measurement of cerebral perfusion with arterial spin labeling: Part 1. Methods. Journal of the International Neuropsychological Society. 2007; 13: 517–525. https://doi.org/10.1017/S1355617707070646

Liu W, Liu J, Bhavsar R, Mao T, Mamikonyan E, Raizen D, et al. Perfusion Imaging of Fatigue and Time-on-Task Effects in Patients With Parkinson's Disease. Frontiers in Aging Neuroscience. 2022; 14: 901203. https://doi.org/10.3389/fnagi.2022.901203

Mackworth JF. Vigilance, arousal, and habituation. Psychological Review. 1968; 75: 308–322. https://doi.org/10.1037/h0025896

Marami B, Scherrer B, Afacan O, Erem B, Warfield SK, Gholipour A. Motion-Robust Diffusion-Weighted Brain MRI Reconstruction Through Slice-Level Registration-Based Motion Tracking. IEEE Transactions on Medical Imaging. 2016; 35: 2258–2269. https://doi.org/10.1109/TMI.2016.2555244

Miller KL, Luh WM, Liu TT, Martinez A, Obata T, Wong EC, et al. Nonlinear temporal dynamics of the cerebral blood flow response. Human Brain Mapping. 2001; 13: 1–12. https://doi.org/10.1002/hbm.1020

Nöth U, Meadows GE, Kotajima F, Deichmann R, Corfield DR, Turner R. Cerebral vascular response to hypercapnia: determination with perfusion MRI at 1.5 and 3.0 Tesla using a pulsed arterial spin labeling technique. Journal of Magnetic Resonance Imaging. 2006; 24: 1229–1235. https://doi.org/10.1002/jmri.20761

Nowinski WL, Fang A, Nguyen BT, Raphel JK, Jagannathan L, Raghavan R, et al. Multiple brain atlas database and atlas-based neuroimaging system. Computer Aided Surgery. 1997; 2: 42–66. https://doi.org/10.1002/(SICI)1097-0150(1997)2:1<42::AID-IGS7>3.0.CO;2-N

Ogawa S, Menon RS, Tank DW, Kim SG, Merkle H, Ellermann JM, et al. Functional brain mapping by blood oxygenation level-dependent contrast magnetic resonance imaging. A comparison of signal characteristics with a biophysical model. Biophysical Journal. 1993; 64: 803–812. https://doi.org/10.1016/S0006-3495(93)81441-3

Olszowy W, Aston J, Rua C, Williams GB. Accurate autocorrelation modeling substantially improves fMRI reliability. Nature Communications. 2019; 10: 1220. https://doi.org/10.1038/s41467-019-09230-w

Pimentel MAF, Vilela P, Sousa I, Figueiredo P. Localization of the hand motor area by arterial spin labeling and blood oxygen level-dependent functional magnetic resonance imaging. Human Brain Mapping. 2013; 34: 96–108. https://doi.org/10.1002/hbm.21418

Pollock JM, Tan H, Kraft RA, Whitlow CT, Burdette JH, Maldjian JA. Arterial spin-labeled MR perfusion imaging: clinical applications. Magnetic Resonance Imaging Clinics of North America. 2009; 17: 315–338. https://doi.org/10.1016/j.mric.2009.01.008

Prodanov D. Data ontology and an information system realization for web-based management of image measurements. Frontiers in Neuroinformatics. 2011; 5: 25. https://doi.org/10.3389/fninf.2011.00025

Raoult H, Petr J, Bannier E, Stamm A, Gauvrit JY, Barillot C, et al. Arterial spin labeling for motor activation mapping at 3T with a 32-channel coil: reproducibility and spatial accuracy in comparison with BOLD fMRI. NeuroImage. 2011; 58: 157–167. https://doi.org/10.1016/j.neuroimage.2011.06.011

Rubia K, Taylor E, Smith AB, Oksanen H, Overmeyer S, Newman S. Neuropsychological analyses of impulsiveness in childhood hyperactivity. The British Journal of Psychiatry. 2001; 179: 138–143. https://doi.org/10.1192/bjp.179.2.138

Salli E, Aronen HJ, Savolainen S, Korvenoja A, Visa A. Contextual clustering for analysis of functional MRI data. IEEE Transactions on Medical Imaging. 2001; 20: 403–414. https://doi.org/10.1109/42.925293

Sourbron S, Ingrisch M, Siefert A, Reiser M, Herrmann K. Quantification of cerebral blood flow, cerebral blood volume, and blood-brain-barrier leakage with DCE-MRI. Magnetic Resonance in Medicine. 2009; 62: 205–217. https://doi.org/10.1002/mrm.22005

Stevenson RA, Geoghegan ML, James TW. Superadditive BOLD activation in superior temporal sulcus with threshold non-speech objects. Experimental Brain Research. 2007; 179: 85–95. https://doi.org/10.1007/s00221-006-0770-6

van Reekum CM, Johnstone T, Urry HL, Thurow ME, Schaefer HS, Alexander AL, et al. Gaze fixations predict brain activation during the voluntary regulation of picture-induced negative affect. NeuroImage. 2007; 36: 1041–1055. https://doi.org/10.1016/j.neuroimage.2007.03.052

Villien M, Chipon E, Troprès I, Bouvier J, Cantin S, Chechin D, et al. Per-subject characterization of bolus width in pulsed arterial spin labeling using bolus turbo sampling. Magnetic Resonance in Medicine. 2013; 69: 1677–1682. https://doi.org/10.1002/mrm.24412

Wang Z, Aguirre GK, Rao H, Wang J, Fernández-Seara MA, Childress AR, et al. Empirical optimization of ASL data analysis using an ASL data processing toolbox: ASLtbx. Magnetic Resonance Imaging. 2008; 26: 261–269. https://doi.org/10.1016/j.mri.2007.07.003

Weber MJ, Detre JA, Thompson-Schill SL, Avants BB. Reproducibility of functional network metrics and network structure: a comparison of task-related BOLD, resting ASL with BOLD contrast, and resting cerebral blood flow. Cognitive, Affective & Behavioral Neuroscience. 2013; 13: 627–640. https://doi.org/10.3758/s13415-013-0181-7

Williams DS, Detre JA, Leigh JS, Koretsky AP. Magnetic resonance imaging of perfusion using spin inversion of arterial water. Proceedings of the National Academy of Sciences of the United States of America. 1992; 89: 212–216. https://doi.org/10.1073/pnas.89.1.212

Wong EC, Buxton RB, Frank LR. Quantitative perfusion imaging using arterial spin labeling. Neuroimaging Clinics of North America. 1999; 9: 333–342.

Wu WC, Mazaheri Y, Wong EC. The effects of flow dispersion and cardiac pulsation in arterial spin labeling. IEEE Transactions on Medical Imaging. 2007; 26: 84–92. https://doi.org/10.1109/TMI.2006.886807

Yang Y, Chang R, Feng X, Li P, Chen Y, Zhang H. An n-Dimensional Chaotic Map with Application in Reversible Data Hiding for Medical Images. Entropy (Basel, Switzerland). 2024; 26: 254. https://doi.org/10.3390/e26030254

Zou Q, Yuan BK, Gu H, Liu D, Wang DJ, Gao JH, et al. Detecting static and dynamic differences between eyes-closed and eyes-open resting states using ASL and BOLD fMRI. PLoS One. 2015; 10: e0121757. https://doi.org/10.1371/journal.pone.0121757